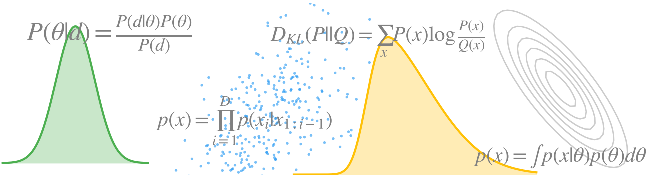

Simulation-Based Inference in Practice

Forward Modelling, Density Estimation, and Testing

Maximilian von Wietersheim-Kramsta

ASTRODAT, Durham University

mwiet.github.io

11th of September 2025

Institute for Computational Cosmology & Centre for Extragalactic Astronomy, Durham University

Simulation-Based Inference (SBI): Contents

SBI: Motivation & Background

Probability of a statement being true given an update to a prior belief and a specific model.

$\Rightarrow$ Bayes' Theorem:

$$P(\boldsymbol{\theta} \mid \boldsymbol{d}) = \frac{P(\boldsymbol{d} \mid \boldsymbol{\theta})\, P(\boldsymbol{\theta})}{P(\boldsymbol{d})} \tag{1}$$

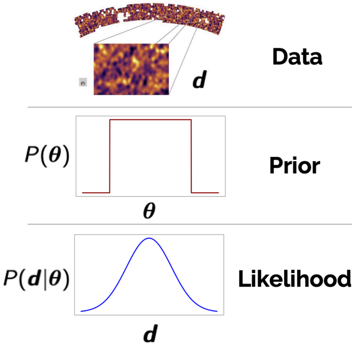

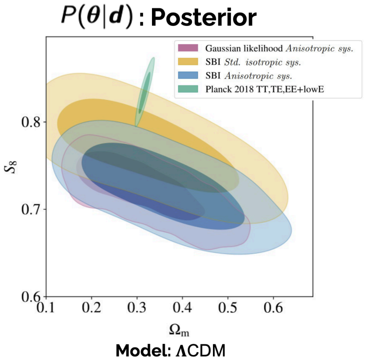

Modelling Likelihood Distributions

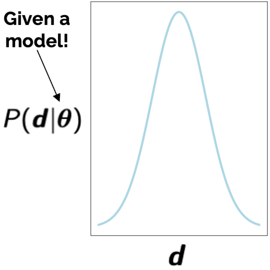

Analytic

e.g. $P(d) \propto \exp\left(-\frac{(d-\mu)^2}{2\sigma^2}\right)$

Modelling Likelihood Distributions

Given a model!

$P(\boldsymbol{d}|\boldsymbol{\theta})$

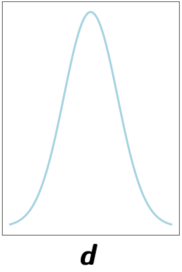

Analytic

e.g. $P(d) \propto \exp\left(-\frac{(d-\mu)^2}{2\sigma^2}\right)$

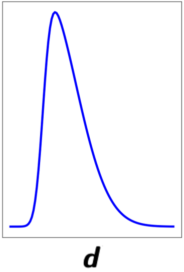

Biased

e.g. Systematics

Modelling Likelihood Distributions

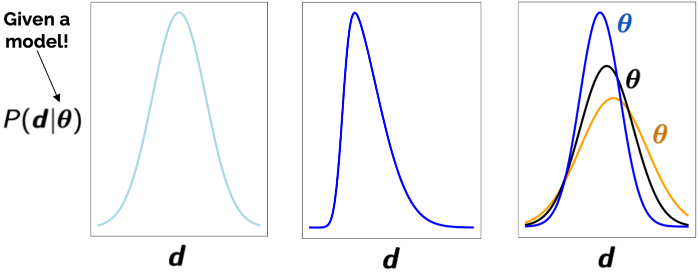

Analytic

e.g. $P(d) \propto \exp\left(-\frac{(d-\mu)^2}{2\sigma^2}\right)$

Biased

e.g. Systematics

Signal-dependent uncertainty

e.g. Non-random noise

Modelling Likelihood Distributions

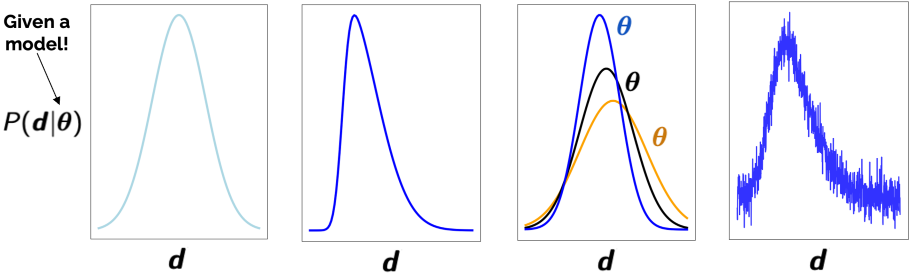

Analytic	Biased	Signal-dependent uncertainty	Intractable
e.g. $P(d) \propto \exp\left(-\frac{(d-\mu)^2}{2\sigma^2}\right)$	e.g. Systematics	e.g. Non-random noise	e.g. Many sources of uncertainty

Zooming Out: the Joint Probability

$$P(\boldsymbol{\theta} \mid \boldsymbol{d}) = \frac{P(\boldsymbol{d} \mid \boldsymbol{\theta})\, P(\boldsymbol{\theta})}{P(\boldsymbol{d})} \propto P(\boldsymbol{\theta}, \boldsymbol{d})\, P(\boldsymbol{\theta}) \tag{2}$$

Joint probability: $P(\boldsymbol{\theta}, \boldsymbol{d} \mid \mathrm{Model})$

Simulator: $\boldsymbol{d}_i \sim P(\boldsymbol{d} \mid \boldsymbol{\theta}, \mathrm{Model})$

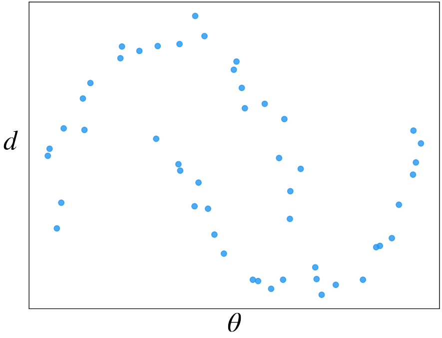

Zooming Out: the Joint Probability

Joint probability: $P(\boldsymbol{\theta}, \boldsymbol{d} \mid \mathrm{Model})$

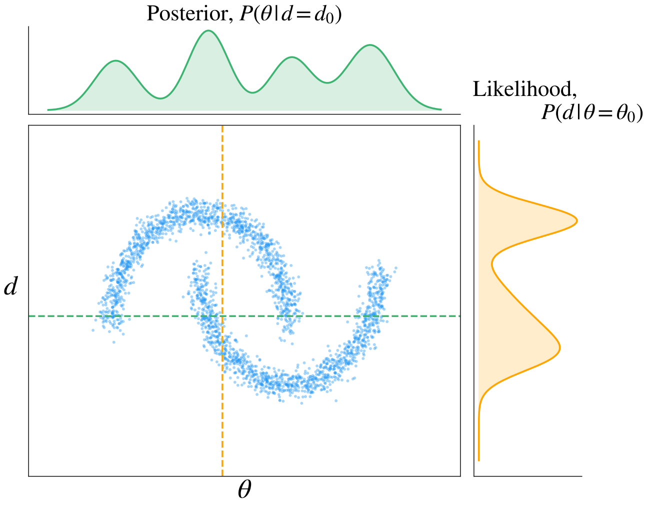

Generalised Bayesian Inference (GBI)

Standard Bayesian inference: Derived from Boolean logic when introducing uncertainty
$\rightarrow$ **Joint probability**, $P(\boldsymbol{\theta}, \boldsymbol{d})$ defines everything for a given model.

Generalised Bayesian Inference: Considers the case of imperfect models $\rightarrow$ Based on Decision theory Berger (2013)
$\rightarrow$ Finds optimal belief given an **imperfect model** and a specific goal
$\rightarrow$ Model is characterised through a **Loss function**, $L(\boldsymbol{\theta}, \boldsymbol{d})$, Bissiri et al. (2013):

$$\underbrace{P_G(\boldsymbol{\theta} \mid \boldsymbol{d})}_{\text{Generalised Posterior}} \propto \underbrace{\exp(-\eta L(\boldsymbol{\theta}, \boldsymbol{d}))}_{\text{Generalised Likelihood}} \times \underbrace{P(\boldsymbol{\theta})}_{\text{Prior}}, \tag{3}$$

where η quantifies the degree of match/mismatch between the data and the model ($\eta = 1$ corresponds to standard Bayes' theorem).
$L(\boldsymbol{\theta}, \boldsymbol{d}) = -\ln P(\boldsymbol{d} \mid \boldsymbol{\theta})$ returns Bayes' theorem.

Simulation-Based Inference

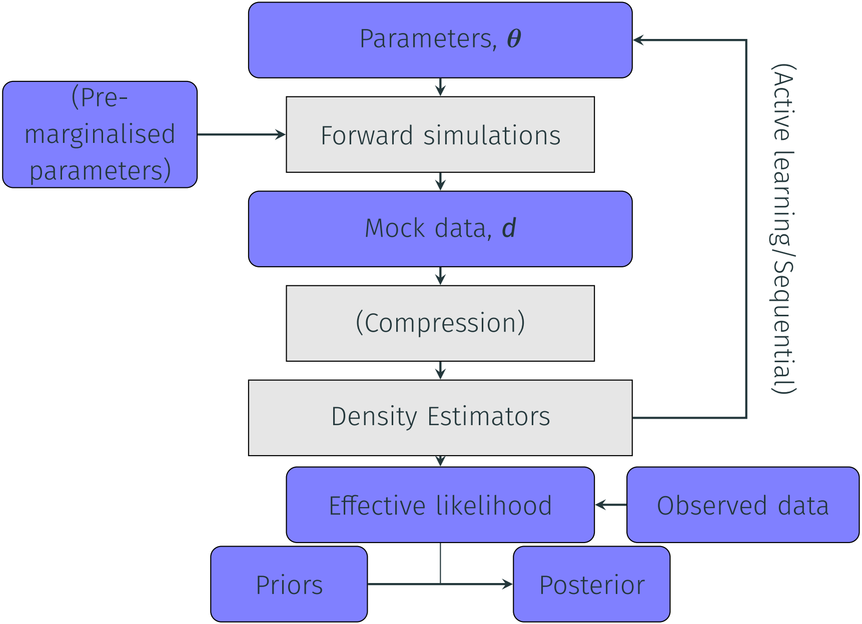

Simulation-Based Inference (SBI) - FAQs

- How do I pick a forward model?
- What type of SBI suits my problem?
- My posterior is robust and reliable, but is my model accurate?
- How do I get the most out of the results of my SBI?

Forward Models

What can we get away with?

1. In what are we interested? - Parameters, model comparison...
2. What is our measurement? - Summary statistics, images...
3. To which systematics will the measurement be sensitive?
4. What type of SBI suits our problem? - NPE, NLE, NRE, active learning...

Forward Models: Capturing the Signal

Complexity

$$C_{\epsilon\epsilon}^{(pq)}(\ell) = C_{\mathrm{gg}}^{(pq)}(\ell) + C_{\mathrm{gI}}^{(pq)}(\ell) + C_{\mathrm{Ig}}^{(pq)}(\ell) + C_{\mathrm{II}}^{(pq)}(\ell)$$

$$C_{ab}^{(pq)}(\ell) = \int_0^\infty \frac{d\chi}{f_k^2(\chi)} W_a^{(p)}(\chi)\, W_b^{(q)}(\chi)\, P_\delta\!\left(\frac{\ell + 1/2}{f_k(\chi)}, \chi\right)$$

$$\tilde{C}_{\epsilon\epsilon,\mu}^{(pq)}(\ell;\mathbf{\Theta}) = \sum_{\ell'=0}^{\ell'_{\max}} \sum_{\ell''=0}^{\ell''_{\max}} \sum_{\nu=1}^{3} \sum_{\nu'=1}^{3} M_{\mu\nu',\ell\ell''} M'^{(pq)}_{\nu'\nu,\ell''\ell'} C_{\epsilon\epsilon,\nu}^{(pq)}(\ell';\mathbf{\Theta})$$

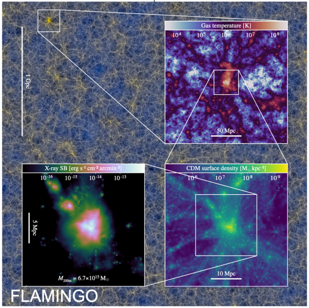

Forward Models: Modelling the Uncertainty

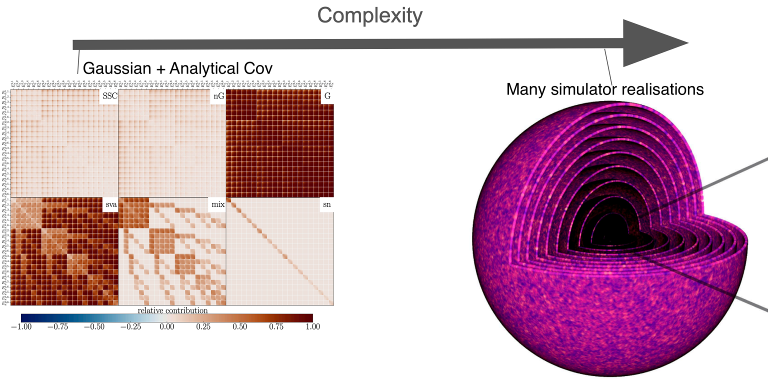

Example: Large-Scale Structure and Weak Lensing

1. Interested in parameter inference of cosmology
2. Measure 2-point statistics $\rightarrow$ Capture 2-point signal and its uncertainty (up to n-point)
3. A range of systematics:
   - Physical: intrinsic alignments, baryonic feedback, (galaxy bias)
   - Observational: photometric redshift uncertainty, masking, galaxy shape calibration uncertainties, anisotropies in the selection function
4. Suited for Neural Likelihood Estimation (only one Universe to observe + prior dependence)

Example: Large-Scale Structure and Weak Lensing

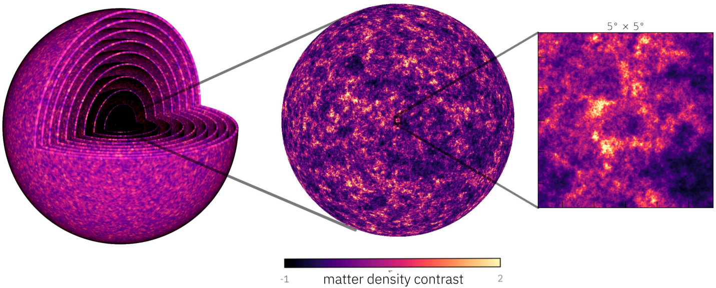

Statistical simulations, e.g. lognormals (Tessore et al., 2023).

Example: Large-Scale Structure and Weak Lensing

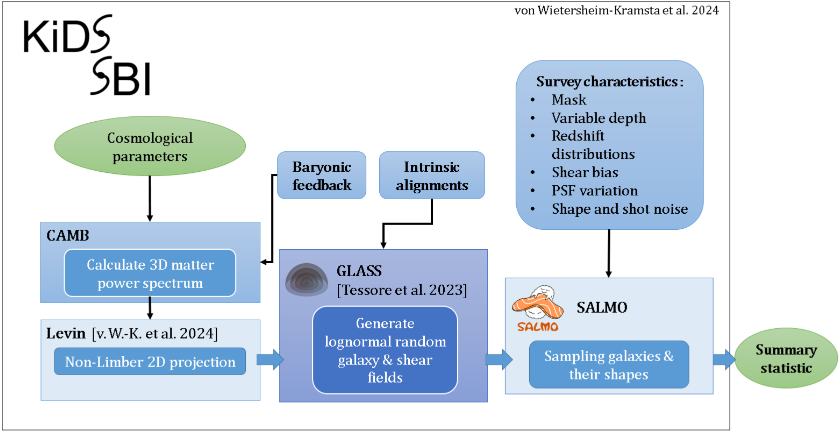

von Wietersheim-Kramsta et al. (2024)

Parameters, Priors, and Pre-Marginalisation

Parameter	Symbol	Prior type	Prior range	Fiducial
Density fluctuation amp.	S_8	Flat	[0.1, 1.3]	0.76
Hubble constant	h_0	Flat	[0.64, 0.82]	0.767
Cold dark matter density	ω_{c}	Flat	[0.051, 0.255]	0.118
Baryonic matter density	ω_{b}	Flat	[0.019, 0.026]	0.026
Scalar spectral index	n_{s}	Flat	[0.84, 1.1]	0.901
Intrinsic alignment amp.	A_{IA}	Flat	[-6, 6]	0.264
Baryon feedback amp.	A_{bary}	Flat	[2, 3.13]	3.1
Redshift displacement	$\boldsymbol{\delta}_z$	Gaussian	$\mathcal{N}(\mathbf{0}, \boldsymbol{C}_z)$	$\mathbf{0}$
Multiplicative shear bias	$M^{(p)}$	Gaussian	$\mathcal{N}(\overline{M}^{(p)}, \sigma_M^{(p)})$	$\overline{M}^{(p)}$
Additive shear bias	$c_{1,2}^{(p)}$	Gaussian	$\mathcal{N}(\overline{c}_{1,2}^{(p)}, \sigma_{c_{1,2}}^{(p)})$	$\overline{c}_{1,2}^{(p)}$
PSF variation shear bias	$\alpha_{1,2}^{(p)}$	Gaussian	$\mathcal{N}(\overline{\alpha}_{1,2}^{(p)}, \sigma_{\alpha_{1,2}}^{(p)})$	$\overline{\alpha}_{1,2}^{(p)}$

von Wietersheim-Kramsta et al. (2024)

Pre-Marginalisation

Pixel

$$\epsilon_{\rm obs}(p, m; \boldsymbol{\Theta}) = \left(1 + M^{(p)}\right)\epsilon_{\rm lensed}(\boldsymbol{\Theta}) + \alpha^{(p)}\epsilon_{\rm PSF}(m) + \cancelto{0}{\beta^{(p)}\delta\epsilon_{\rm PSF}} + c^{(p)}$$

Tomographic bin

Multiplicative shear bias

PSF shear bias

Additive shear bias

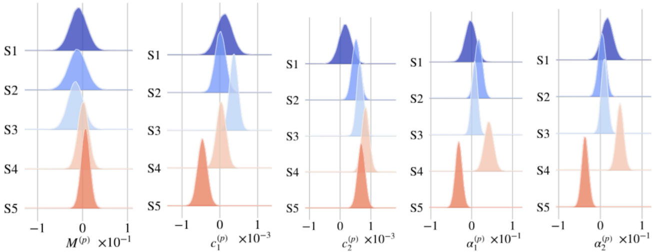

von Wietersheim-Kramsta et al. (2024)

Example: Galaxy-Scale Strong Lensing

1. Interested in parameter inference of cosmology and model comparison between dark matter models

2. Observe full images of lenses

3. A range of systematics:
   - Physical: external shear, multipoles, lens light, source complexity, etc.
   - Observational: point-spread function, pixel noise, selection effects, resolution, etc.

4. Suited for Neural Posterior Estimation (many lenses which can be amortised)

Frame Title

Source:
- Elliptical Core-Sersic
- z = 1
- **Axis ratio ∈ [0.3, 0.85)**
- **Axial tilt ∈ [30, 70]°**

Lens:
- Power law mass
- z = 0.5
- No external shear
- **R_E ∈ [1.0, 1.5]”**

Perturbers:
- Warm Dark Matter
- Truncated NFW mass
- $M_{hf} = 10^7$
- **$n_{subhalos}$ ∈ [0, 30]**

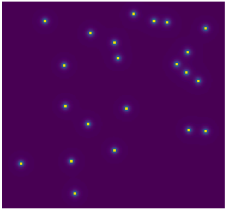

He et al. (2022), von Wietersheim-Kramsta et al. (in prep.)

Observational Effects (HST-like)
- Exposure = 8000s
- Sky background = 0.1
- Pixel scale = 0.05”
- σ_{PSF} = 0.05”
- + Poisson noise

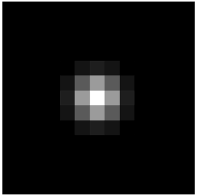

Frame Title

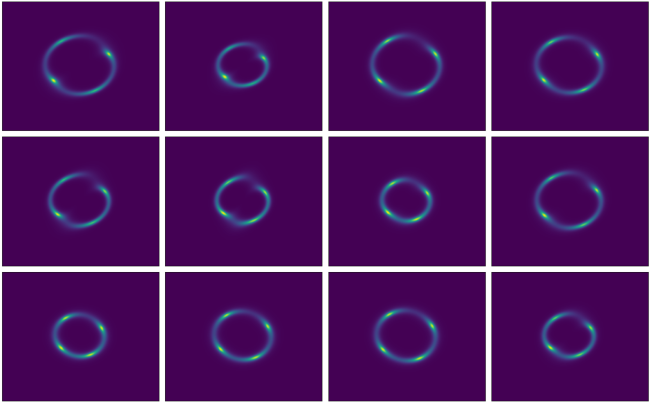

von Wietersheim-Kramsta et al. (in prep.)

Types of SBI

Types of Simulation-Based Inference

a.k.a. Likelihood-free or implicit likelihood inference

- Approximate Bayesian Computation (ABC)
- Neural Density Estimation (NDE)
  - Neural Posterior Estimation (NPE)
  - Neural Likelihood Estimation (NLE)
  - Neural Ratio Estimation (NRE)
  - Neural Posterior Score Estimation (NPSE)
- Sequential Methods

Simplest Case: Approximate Bayesian Computation

1. Draw simulations from simulator within prior space:

$$\boldsymbol{d}^* \sim P(\boldsymbol{d} \mid \boldsymbol{\theta}^*);\ \ \boldsymbol{\theta}^* \sim P(\boldsymbol{\theta}). \tag{4}$$

2. Define a distance metric between simulated data, $\boldsymbol{d}^*$, and observed data, $\boldsymbol{d}_0$ (e.g. Euclidean):

$$D = D(\boldsymbol{d}_0,\ \boldsymbol{d}^*). \tag{5}$$

3. Accept or reject according to arbitrary threshold, ϵ and repeat Rubin (1984):

$$\mathrm{if}\, D < \epsilon, \mathrm{keep}\, \boldsymbol{\theta}^*. \tag{6}$$

In the context of GBI, the Loss function is:

$$L(\boldsymbol{\theta}, \boldsymbol{d}) = \begin{cases} 0, & \text{if } D < \epsilon, \\ \infty, & \text{otherwise.} \end{cases} \tag{7}$$

Simplest Case: Approximate Bayesian Computation

Converges given:

$$\lim_{\epsilon \to 0} P_{\mathrm{ABC}}(\theta \mid d_0) = P(\theta \mid d_0). \quad (8)$$

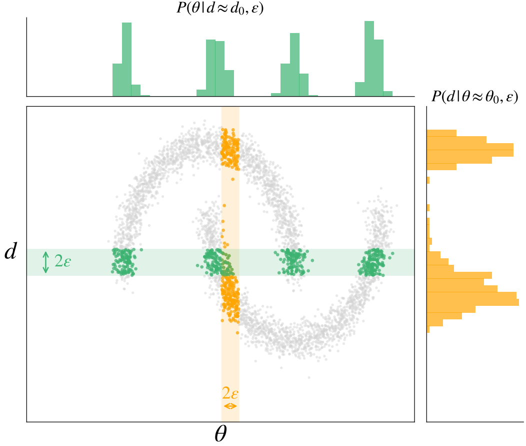

Simplest Case: Approximate Bayesian Computation

- **Curse of Dimensionality**: Performance degrades significantly with the dimensionality the data vector and model.
- Requires significant **compression**.
- The results sensitive to the choice of distance metric and ϵ.
- **Inefficiency**: Large number of simulations may be rejected, especially for small ϵ.
- **Not amortised**: Reevaluation required for each new d_0.
- **Recent applications**: e.g. galaxy morphology (Cameron and Pettitt, 2012; Tortorelli et al., 2021), diffuse X-ray background (Baxter et al., 2022), galaxy-scale strong lenses (He et al., 2022)

Neural Posterior Estimation (NPE)

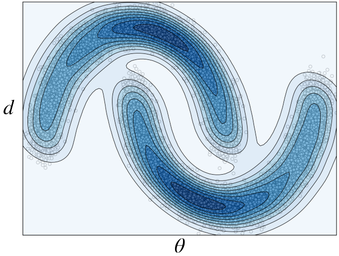

$D_{KL}(P \mid\mid Q) = \sum_x P(x) \log \frac{P(x)}{Q(x)}$

See Papamakarios and Murray (2016); Lueckmann et al. (2017); Greenberg et al. (2019); Cranmer et al. (2020)

1. Draw simulations:

$$\boldsymbol{d}^* \sim P(\boldsymbol{d} \mid \boldsymbol{\theta}^*); \; \boldsymbol{\theta}^* \sim P(\boldsymbol{\theta}). \tag{9}$$

2. Find an estimator of the posterior, $\hat{P}_w(\boldsymbol{\theta} \mid \boldsymbol{d})$, with its weights, $\boldsymbol{w}$, such that:

$$\boldsymbol{w}^* = \arg\min_w \mathbb{E}_{P(\boldsymbol{d})}[\, D_{\mathrm{KL}}(P(\boldsymbol{\theta} \mid \boldsymbol{d}) \mid\mid \hat{P}_w(\boldsymbol{\theta} \mid \boldsymbol{d}))], \tag{10}$$

$$\boldsymbol{w}^* = \arg\max_w \mathbb{E}_{P(\boldsymbol{\theta},\boldsymbol{d})}[\, \ln(\hat{P}_w(\boldsymbol{\theta} \mid \boldsymbol{d}))]. \tag{11}$$

3. Train a neural network from this loss function:

$$L(\boldsymbol{w}) = -\mathbb{E}_{P(\boldsymbol{\theta},\boldsymbol{d})}[\, \ln(\hat{P}_w(\boldsymbol{\theta} \mid \boldsymbol{d}))] \tag{12}$$

4. Use network to directly sample $\hat{P}_w(\boldsymbol{\theta} \mid \boldsymbol{d})$.

Neural Posterior Estimation (NPE)

- **Amortised***: Direct mapping from $\boldsymbol{d}$ to $P(\boldsymbol{\theta} \mid \boldsymbol{d})$.
- ***Amortisation gap**: If observed data, d_0, changes, $\hat{P}_w(\boldsymbol{\theta} \mid \boldsymbol{d})$ may not be well characterised at new $d_0 \rightarrow$ Additional training required.
- ***Prior-dependent**: For new parameters priors, retraining is necessary.
- **Recent applications**: e.g. galaxy clustering (Lemos et al., 2023b), exoplanets (Vasist et al., 2023), gravitational waves (Leyde et al., 2024), X-ray spectra (Barret and Dupourqué, 2024), lensed quasars (Erickson et al., 2024)
- **Implemented in**: `sbi` (Tejero-Cantero et al., 2020), `lampe` (Rozet et al., 2021) and `ltu-ili` (Ho et al., 2024).

Neural Likelihood Estimation (NLE)

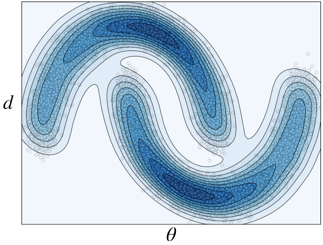

$D_{KL}(P||Q) = \sum_x P(x) \log \frac{P(x)}{Q(x)}$

See Papamakarios and Murray (2016); Papamakarios et al. (2017); Alsing et al. (2019); Cranmer et al. (2020); Boelts et al. (2022); Glöckler et al. (2022)

1. Draw simulations:
$$\boldsymbol{d}^* \sim P(\boldsymbol{d} \mid \boldsymbol{\theta}^*); \;\; \boldsymbol{\theta}^* \sim P(\boldsymbol{\theta}). \tag{13}$$

2. Find an estimator of the likelihood, $\hat{P}_w(\boldsymbol{d} \mid \boldsymbol{\theta})$, with its weights, $\boldsymbol{w}$, such that:
$$\boldsymbol{w}^* = \arg\min_w \mathbb{E}_{P(\boldsymbol{d})}\left[D_{\mathrm{KL}}(P(\boldsymbol{d} \mid \boldsymbol{\theta}) \,||\, \hat{P}_w(\boldsymbol{d}|\boldsymbol{\theta}))\right], \tag{14}$$
$$\boldsymbol{w}^* = \arg\max_w \mathbb{E}_{P(\boldsymbol{\theta},\boldsymbol{d})}\left[\ln(\hat{P}_w(\boldsymbol{d}|\boldsymbol{\theta}))\right]. \tag{15}$$

3. Train a neural network from this loss function:
$$L(\boldsymbol{w}) = -\mathbb{E}_{P(\boldsymbol{\theta},\boldsymbol{d})}\left[\ln(\hat{P}_w(\boldsymbol{d}|\boldsymbol{\theta}))\right]. \tag{16}$$

4. Define priors, $P(\boldsymbol{\theta})$, and sample posterior with an MCMC.

Neural Likelihood Estimation (NLE)

- **Prior-independent**: Learnt likelihood can be reused for sampling when varying the priors.
- **Useful for model testing**: Likelihood evaluation allows for model comparison.
- **Sampling required**: Requires sampling with MCMC or other sampler to obtain posteriors.
- **Compression**: Can struggle with high-dimensional data $\rightarrow$ Requiring compression.
- **Recent applications**: e.g. weak lensing (Jeffrey et al., 2024; von Wietersheim-Kramsta et al., 2024), seismology (Saoulis et al., 2025)
- **Implemented in**: `sbi` (Tejero-Cantero et al., 2020), `delfi` (Alsing et al., 2019) and `ltu-ili` (Ho et al., 2024).

NDE: Normalising Flows

- Used for **NPE** and **NLE**, as they naturally encode the normalisation of the probability densities (Papamakarios et al., 2021).
- Learns **invertible and differentiable** transformations between any distribution and a Gaussian.
- Usually train ensembles in parallel for robustness.
- Examples: Masked Autoregressive Flows (MAF), Neural Spline Flows (NSF), etc.

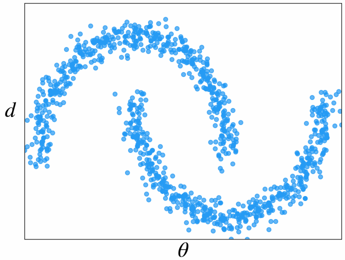

Neural Ratio Estimation (NRE)

1. Typically, learn the likelihood-to-evidence:

$$r(\boldsymbol{d} \mid \boldsymbol{\theta}) = P(\boldsymbol{d} \mid \boldsymbol{\theta})/P(\boldsymbol{d}) = P(\boldsymbol{\theta} \mid \boldsymbol{d})/P(\boldsymbol{\theta}). \tag{17}$$

2. Train a neural classifier, $Q_w(\boldsymbol{d}, \boldsymbol{\theta})$, to distinguish draws from:
   - The "true" joint distribution $P(\boldsymbol{d}, \boldsymbol{\theta}) = P(\boldsymbol{d} \mid \boldsymbol{\theta})\, P(\boldsymbol{\theta})$.
   - The product of the marginal distributions $P(\boldsymbol{d})\, P(\boldsymbol{\theta})$.
3. When optimised, we find:

$$Q^*(\boldsymbol{d}, \boldsymbol{\theta}) = P(\boldsymbol{d}, \theta)/[P(\boldsymbol{d}, \boldsymbol{\theta}) + P(\boldsymbol{d})P(\boldsymbol{\theta})]. \tag{18}$$

$$\hat{r}(\boldsymbol{d} \mid \boldsymbol{\theta}) = \frac{Q_w(\boldsymbol{d}, \boldsymbol{\theta})}{1 - Q_w(\boldsymbol{d}, \boldsymbol{\theta})} \approx \frac{P(\boldsymbol{d} \mid \boldsymbol{\theta})}{P(\boldsymbol{d})}. \tag{19}$$

4. Sample posterior from $P(\boldsymbol{\theta} \mid \boldsymbol{d}_0) \propto \hat{r}(\boldsymbol{d}_0 \mid \boldsymbol{\theta})P(\boldsymbol{\theta})$.

See Hermans et al. (2019); Cranmer et al. (2020); Durkan et al. (2020); Delaunoy et al. (2022); Miller et al. (2022)

Neural Ratio Estimation (NRE)

- **Robust ratio estimates**: Useful to directly compute likelihood ratios for model testing.
- **Scalability**: Can scale well in high-dimensional parameter spaces, e.g. Truncated Marginal Neural Ratio Estimation (TMNRE).
- **Density-Chasm problem**: joint distribution and marginal distributions may have little overlap in high dimensions.
- **Recent applications**: e.g. CMB (Cole et al., 2022), strong lensing (Anau Montel et al., 2023; Filipp et al., 2024), pulsars (Berteaud et al., 2024), supernova cosmology (Karchev and Trotta, 2024)
- **Implemented in**: `sbi` (Tejero-Cantero et al., 2020), `swyft` (Miller et al., 2022) and `ltu-ili` (Ho et al., 2024).

Sequential SBI and Active Learning

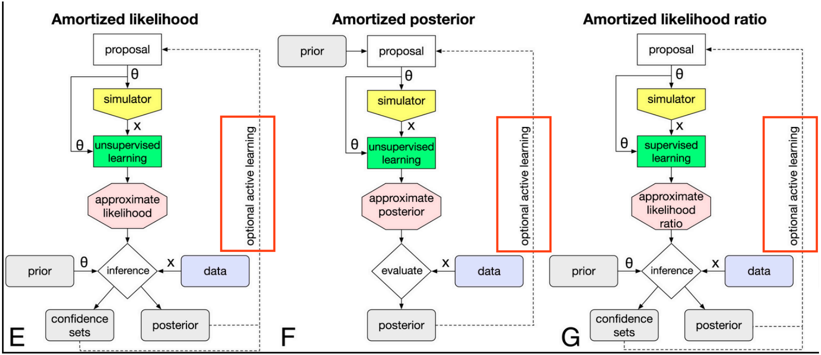

Cranmer et al. (2020)

Sequential SBI and Active Learning

1. Draw initial simulations, $(\boldsymbol{\theta}_i, \boldsymbol{d}_i)$.

2. Train initial density estimate $\hat{P}_{w^{(1)}}(\boldsymbol{\theta} \mid \boldsymbol{x})$ or $\hat{P}_{w^{(1)}}(\boldsymbol{d} \mid \boldsymbol{\theta})$.

3. For subsequent rounds $r > 1$, construct a proposal distribution, $\tilde{P}^{(r)}(\theta)$; e.g., $\tilde{P}^{(r)}(\boldsymbol{\theta}) \propto \hat{P}_{w^{(r-1)}}(\boldsymbol{\theta} \mid \boldsymbol{d}_0)$.

4. Draw new simulations with $\boldsymbol{\theta}_j \sim \tilde{P}^{(r)}(\boldsymbol{\theta})$ and $\boldsymbol{d}_j \sim P(\boldsymbol{d} \mid \boldsymbol{\theta}_j)$.

5. Retrain the density estimator using all accumulated simulations.

Going to Higher Dimensions

Neural Posterior Score Estimation (NPSE)

1. Directly estimates the score of the posterior (or likelihood):

$$s(\boldsymbol{\theta} \mid \boldsymbol{d}) = \nabla_{\boldsymbol{\theta}} \ln P(\boldsymbol{\theta} \mid \boldsymbol{d}). \tag{20}$$

2. “Forward” noising process perturbs samples from the target distribution with noise.
3. A network, $s_w(\boldsymbol{\theta}, \boldsymbol{d}, t)$, is trained to estimate the score of the distributions at different noise levels, t (e.g. with denoising score matching), such that:

$$s_w(\boldsymbol{\theta}, \boldsymbol{d}_0, t) \approx \nabla_{\boldsymbol{\theta}} \ln P_t(\boldsymbol{\theta} \mid \boldsymbol{d}_0). \tag{21}$$

4. Sample posterior by either inverting the network or using Langevin MCMC.

See Hyvärinen and Dayan (2005); Sharrock et al. (2022)

Neural Posterior Score Estimation (NPSE)

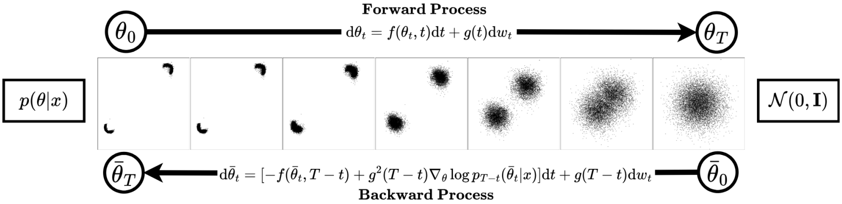

Sharrock et al. (2022)

- **Flexible** network architecture, without normalisation requirements (e.g. diffusion models).
- Should scale well to **high-dimensional** data/parameter spaces.
- Naturally incorporates **gradients**.
- Still untested in many contexts.

Flow Matching Posterior Estimation (FMPE)

1. A continuous normalising flow is used to maps from $q_0(\theta|x)$, to a target posterior distribution, $q(\theta|x)$, parameterised by $t \in [0, 1]$ continuously. The flow is defined by a velocity vector field of trajectories. The continuous trajectory, ψ, of a sample θ is determined by the ODE:

$$\frac{d}{dt}\psi_{t,x}(\theta) = v_{t,x}[\psi_{t,x}(\theta)], \quad \psi_{0,x}(\theta) = \theta. \tag{22}$$

2. Find an optimal transport sample-conditional probability path.
3. Train the neural network that parameterises the vector field, $v_{t,x}$, by minimising the difference between $v_{t,x}$ and the target, u_t:

$$\mathcal{L} = \mathbb{E}_{t\sim p(t),\theta_1\sim p(\theta),x\sim p(x|\theta_1),\theta_t\sim p_t(\theta_t|\theta_1)}||v_{t,x}(\theta_t) - u_t(\theta_t|\theta_1)||^2. \tag{23}$$

See Wildberger et al. (2023)

Flow Matching Posterior Estimation (FMPE)

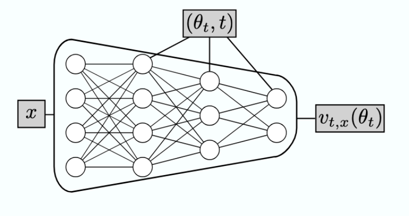

Wildberger et al. (2023)

- **Flexible** network architecture.
- Should scale well to **high-dimensional** data/parameter spaces.
- Provides direct access to the posterior density like NPE (**no sampler required**).
- Uses deterministic ODEs $\rightarrow$ Exact density evaluation. While NPSE is based on stochastic DE $\rightarrow$ Sampling needed.
- Fast training, but slower inference.

Data Compression

Data Compression: Linear vs. Non-Linear Compression

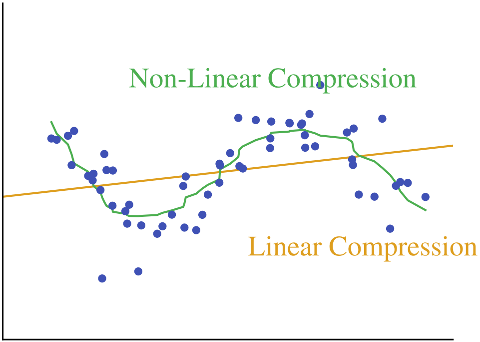

- **Linear methods** may loose non-Gaussian and non-linear information. Sometimes also require an analytic likelihood.

- **Non-linear methods** can address this, but can come at the expense of efficiency and interpretability.

Data Compression: Linear Compression

- **Principal Component Analysis** (PCA): Projects data onto principal components capturing maximal variance (e.g. Barret and Dupourqué 2024).
- **Canonical Correlation Analysis** (CCA): Finds linear combinations of two sets of model parameters, $\boldsymbol{\theta}$, and data, $\boldsymbol{d}$, that are maximally correlated (e.g. Park et al. 2025).
- **Score Compression**: Utilises the score function (gradient of the log-likelihood with respect to parameters, $\nabla_{\boldsymbol{\theta}} \ln P(\boldsymbol{d} \mid \boldsymbol{\theta})$), for compression. Can be lossless in Fisher information (Alsing and Wandelt, 2018).
- **MOPED** and **e-MOPED**: Lossless compression in Fisher information under Gaussian likelihood assumption (Heavens et al., 2000).

Linear Compression: Score Compression in Weak Lensing

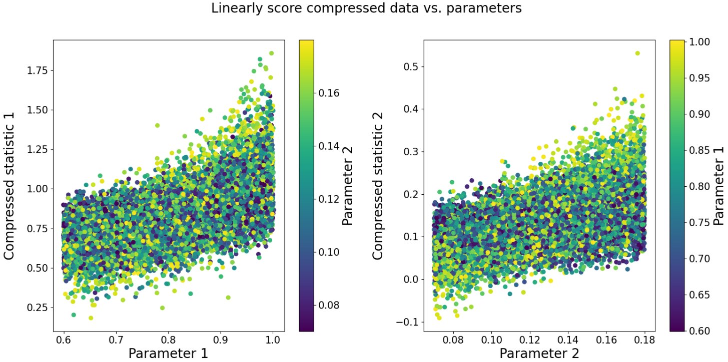

Alsing et al. (2018); Lin et al. (2023); von Wietersheim-Kramsta et al. (2024)

$$t = \nabla d$$

Linear Compression: Score Compression in Weak Lensing

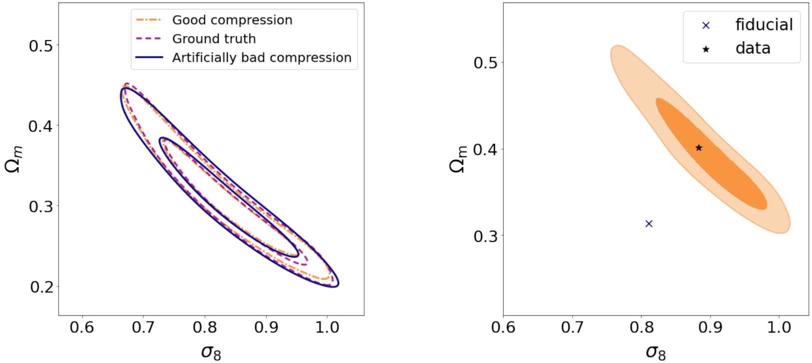

Lin et al. (2023); von Wietersheim-Kramsta et al. (2024)

Data Compression: Non-Linear Compression

- **Deep Auto-Enconders**: Unsupervised neural networks consisting of an encoder that maps data to a lower dimensional space.
- **Convolutional Neural Networks** (CNN): Type of encoder that involves filter/kernel optimization (e.g. Lemos et al. 2023b; Jeffrey et al. 2024).
- **Information-Maximising Neural Networks**: Compress with neural networks which find non-linear summary statistics that explicitly maximising the Fisher information (e.g. Charnock et al. 2018; Makinen et al. 2025).

Can all be an embedding.

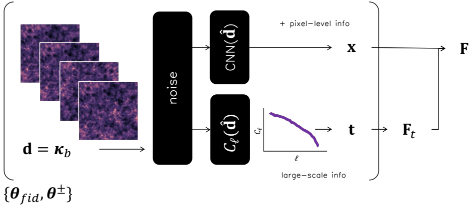

Example: IMNN Hybrid Summaries in Strong Lensing

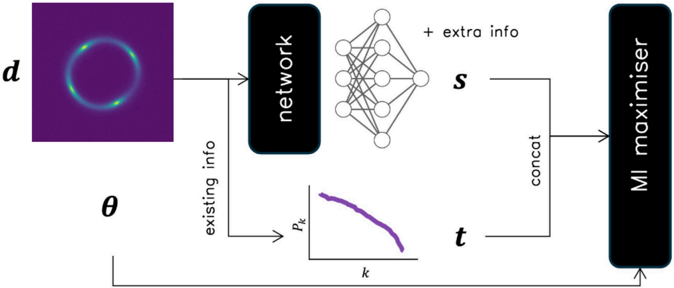

Makinen et al. (2025)

Example: IMNN Hybrid Summaries in Strong Lensing

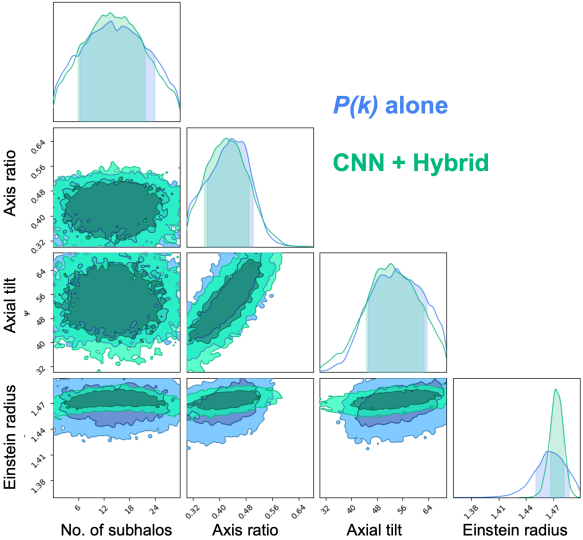

von Wietersheim-Kramsta et al. (in prep.)

Model Testing & Misspecification with SBI

Bayesian Model Testing

For a given model, $\mathcal{M}$, and observed data, d, the **Bayesian evidence**, $P(d \mid \mathcal{M})$, is defined as :

$$P(d \mid \mathcal{M}) = \int P(d \mid \theta, \mathcal{M})\, P(\theta \mid \mathcal{M})\, d\theta. \tag{24}$$

When comparing two models, $\mathcal{M}_1$ and $\mathcal{M}_2$, one may define the **Bayes factor**:

$$B_{12} = \frac{P(d \mid \mathcal{M}_1)}{P(d \mid \mathcal{M}_2)}. \tag{25}$$

$\rightarrow$ Ratio of posterior odds to prior odds of the two models and provides a measure of the evidence in favor of $\mathcal{M}_1$ over $\mathcal{M}_2$.

Naturally incorporates Occam's razor: overly complex models are disfavoured.

Bayesian Model Testing with SBI

- **NLE-based**: Integrate the learnt likelihood.
- **NLE/NPE or NRE**: If all are available, can compute $\hat{P}(d|\mathcal{M}) \approx \frac{\hat{P}_{w'}(d|\theta_0,\mathcal{M})\,P(\theta_0|\mathcal{M})}{\hat{P}_w(\theta_0|d,\mathcal{M})}$ (Spurio Mancini et al., 2023).
- **floZ**: Training a normalising flow directly on the evidence (Srinivasan et al., 2024).
- **Classifier-based**: Train classifier to distinguish $d \sim \mathcal{M}_1$ from $d \sim \mathcal{M}_2$ (e.g. Jeffrey and Wandelt 2024).

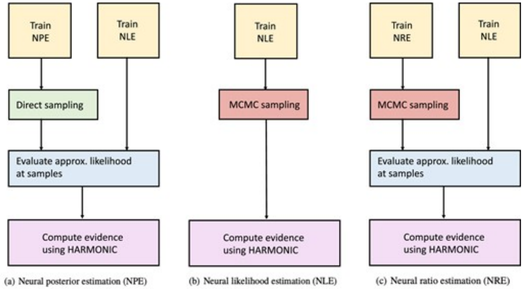

Spurio Mancini et al. (2023)

Model Misspecification in SBI

- Model misspecification can cause **biased posterior estimates** despite a self-consistent SBI.
- **Excessive extrapolation:** If the observed data is out-of-distribution (OOD), the trained NNs are no longer describing the correct probability distribution.
- **Mitigation**:
  - GBI framing
  - Error modelling within NDE (Huang et al., 2023; Kelly et al., 2025)
  - Ensembling

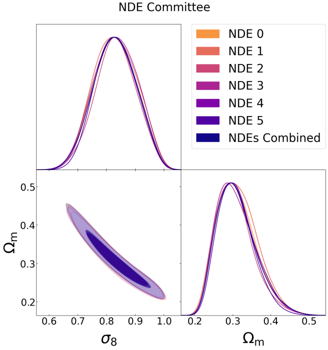

Lin et al. (2023)

Diagnosing & Testing SBI

Convergence of Training

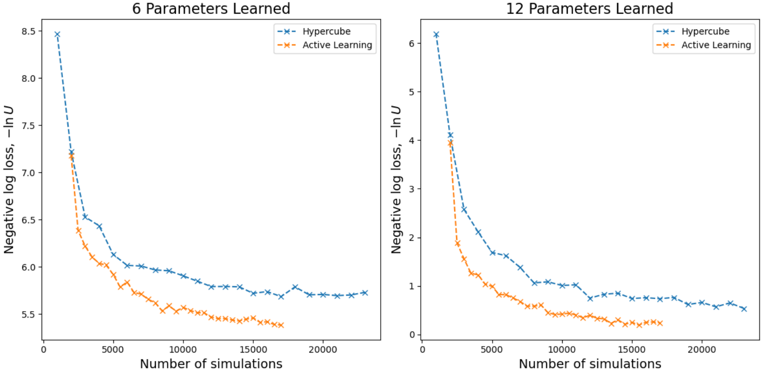

Lin et al. (2023); von Wietersheim-Kramsta et al. (2024)

Testing for OOD: Goodness-of-Fit Tests

$$\chi^2(\boldsymbol{d}|\boldsymbol{\Theta}) = (\boldsymbol{d}_i - \mathrm{E}[\boldsymbol{d}_*|\boldsymbol{\Theta}_*])^{\mathrm{T}}(\mathrm{Cov}(\boldsymbol{d}_*|\boldsymbol{\Theta}_*))^{-1}(\boldsymbol{d}_i - \mathrm{E}[\boldsymbol{d}_*|\boldsymbol{\Theta}_*]) \tag{26}$$

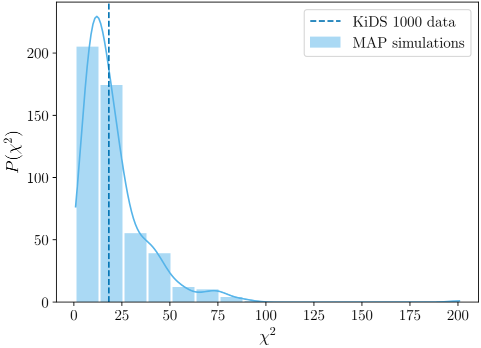

GoF measure under Gaussian likelihood assumption (von Wietersheim-Kramsta et al., 2024)

Testing for OOD: Goodness-of-Fit Tests

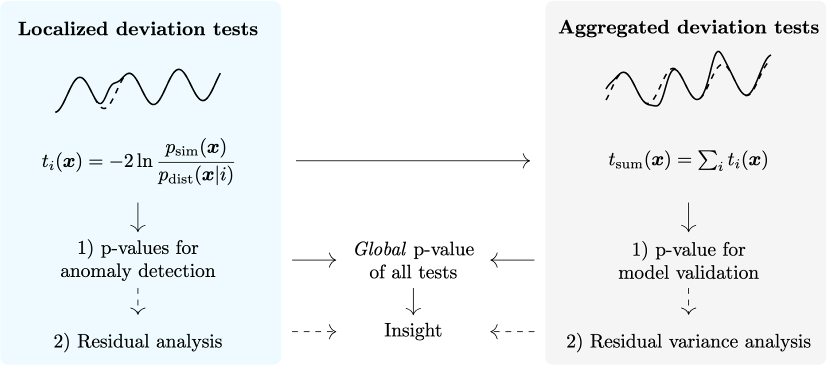

Posterior predictive tests (Anau Montel et al., 2025)

Testing for OOD: Goodness-of-Fit Tests

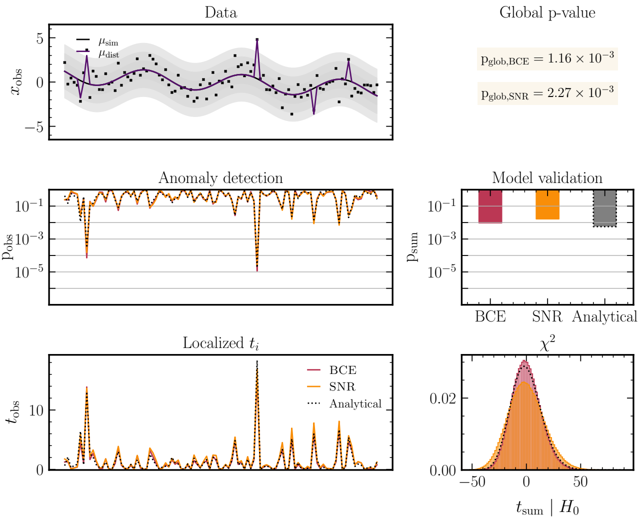

Posterior predictive tests (Anau Montel et al., 2025)

Consistency between SBI & Simulator: Simulation-Based Calibration

1. For a fixed θ^*, draw N posterior samples, θ_i.
2. Evaluate the probability that the true parameter * is less than some drawn value, according to the recovered posterior (i.e. the rank).
3. Averaging over many simulations, we evaluate the posterior cumulative density distribution.

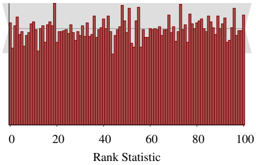

Accurate posterior

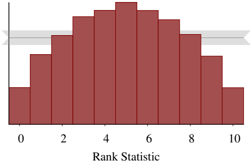

Learnt posterior too wide

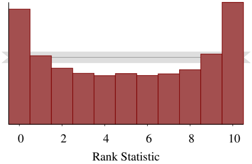

Learnt posterior to narrow

Simulation-Based Calibration (Talts et al., 2018). Available in `ltu-ili`.

Consistency between SBI & Simulator: Coverage/TARP

1. Draw parameter samples from the learnt posterior.
2. Run forward simulations at the parameters.
3. Evaluate fraction (f) of parameter samples per sim (i) where: $P(\theta_i|d_i) < P(\theta_i^*|d_i)$.
4. Evaluate fraction of sims where f is within the expected fraction.

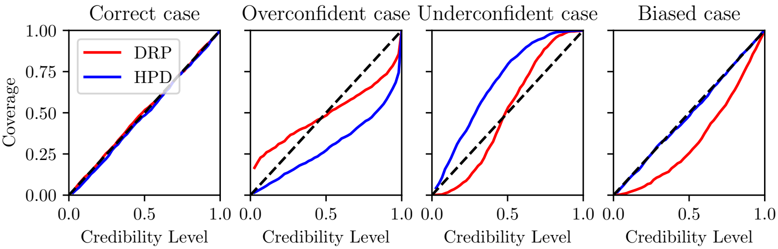

Coverage tests/TARP (Deistler et al., 2022; Lemos et al., 2023a). Available in `ltu-ili`.

Examples: TARP in Weak and Strong Lensing SBI

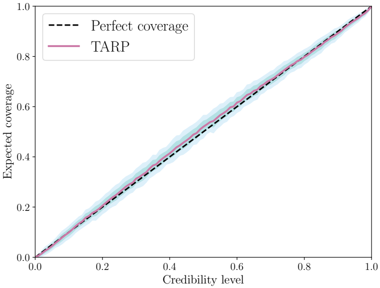

von Wietersheim-Kramsta et al. (2024)

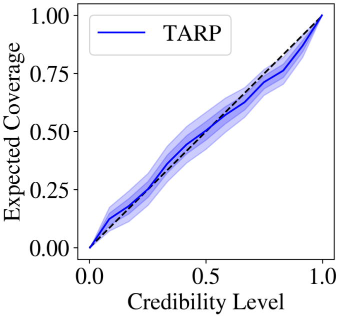

von Wietersheim-Kramsta, et al. (in prep.)

Conclusion & Outlooks

Outlooks

- SBI is a powerful method allowing for increasingly complex modelling.
- Some **caveats** $\rightarrow$ Extensive testing and validation required.
- Still limited by computational resources, particularly, with higher dimensional data.

- **Future avenues**:
  - Neural Posterior Score Estimation (NPSE) and Flow Matching Posterior Estimation (FMPE)
  - Transfer Learning to combine constraints
  - Training with multifidelity simulators (Krouglova et al., 2025)
- **Exenstive applications**: large datasets from surveys, simulations and high-resolution imaging.

Questions?

References

Alsing, J., Charnock, T., Feeney, S., and Wandelt, B. (2019). Fast likelihood-free cosmology with neural density estimators and active learning. *Monthly Notices of the Royal Astronomical Society*, 488(3):4440–4458.

Alsing, J. and Wandelt, B. (2018). Generalized massive optimal data compression. , 476(1):L60–L64.

Alsing, J., Wandelt, B., and Feeney, S. (2018). Massive optimal data compression and density estimation for scalable, likelihood-free inference in cosmology. *Monthly Notices of the Royal Astronomical Society*, 477(3):2874–2885.

Anau Montel, N., Alvey, J., and Weniger, C. (2025). Tests for model misspecification in simulation-based inference: From local distortions to global model checks. , 111(8):083013.

Anau Montel, N., Coogan, A., Correa, C., Karchev, K., and Weniger, C. (2023). Estimating the warm dark matter mass from strong lensing images with truncated marginal neural ratio estimation. , 518(2):2746–2760.

Barret, D. and Dupourqué, S. (2024). Simulation-based inference with neural posterior estimation applied to X-ray spectral fitting. Demonstration of working principles down to the Poisson regime. , 686:A133.

Baxter, E. J., Christy, J. G., and Kumar, J. (2022). Approximate Bayesian Computation applied to the Diffuse Gamma-Ray Sky. , 516(2):2326–2336.

Berger, J. O. (2013). *Statistical decision theory and Bayesian analysis*. Springer Science & Business Media.

Berteaud, J., Eckner, C., Calore, F., Clavel, M., and Haggard, D. (2024). Simulation-based Inference of Radio Millisecond Pulsars in Globular Clusters. , 974(1):144.

Bissiri, P. G., Holmes, C., and Walker, S. (2013). A General Framework for Updating Belief Distributions. *arXiv e-prints*, page arXiv:1306.6430.

Boelts, J., Lueckmann, J.-M., Gao, R., and Macke, J. H. (2022). Flexible and efficient simulation-based inference for models of decision-making. *eLife*, 11:e77220.

Cameron, E. and Pettitt, A. N. (2012). Approximate Bayesian Computation for astronomical model analysis: a case study in galaxy demographics and morphological transformation at high redshift. , 425(1):44–65.

References iv

Charnock, T., Lavaux, G., and Wandelt, B. D. (2018). Automatic physical inference with information maximizing neural networks. , 97(8):083004.

Cole, A., Miller, B. K., Witte, S. J., Cai, M. X., Grootes, M. W., Nattino, F., and Weniger, C. (2022). Fast and credible likelihood-free cosmology with truncated marginal neural ratio estimation. , 2022(9):004.

Cranmer, K., Brehmer, J., and Louppe, G. (2020). The frontier of simulation-based inference. *Proceedings of the National Academy of Science*, 117(48):30055–30062.

Deistler, M., Goncalves, P. J., and Macke, J. H. (2022). Truncated proposals for scalable and hassle-free simulation-based inference. *arXiv e-prints*, page arXiv:2210.04815.

References v

Delaunoy, A., Hermans, J., Rozet, F., Wehenkel, A., and Louppe, G. (2022). Towards Reliable Simulation-Based Inference with Balanced Neural Ratio Estimation. *arXiv e-prints*, page arXiv:2208.13624.

Durkan, C., Murray, I., and Papamakarios, G. (2020). On Contrastive Learning for Likelihood-free Inference. *arXiv e-prints*, page arXiv:2002.03712.

Erickson, S., Wagner-Carena, S., Marshall, P., Millon, M., Birrer, S., Roodman, A., Schmidt, T., Treu, T., Schuldt, S., Shajib, A., Venkatraman, P., and The LSST Dark Energy Science Collaboration (2024). Lens Modeling of STRIDES Strongly Lensed Quasars using Neural Posterior Estimation. *arXiv e-prints*, page arXiv:2410.10123.

Filipp, A., Hezaveh, Y., and Perreault-Levasseur, L. (2024). Robustness of Neural Ratio and Posterior Estimators to Distributional Shifts for Population-Level Dark Matter Analysis in Strong Gravitational Lensing. *arXiv e-prints*, page arXiv:2411.05905.

Glöckler, M., Deistler, M., and Macke, J. H. (2022). Variational methods for simulation-based inference. *arXiv e-prints*, page arXiv:2203.04176.

Greenberg, D. S., Nonnenmacher, M., and Macke, J. H. (2019). Automatic Posterior Transformation for Likelihood-Free Inference. *arXiv e-prints*, page arXiv:1905.07488.

He, Q., Robertson, A., Nightingale, J., Cole, S., Frenk, C. S., Massey, R., Amvrosiadis, A., Li, R., Cao, X., and Etherington, A. (2022). A forward-modelling method to infer the dark matter particle mass from strong gravitational lenses. , 511(2):3046–3062.

Heavens, A. F., Jimenez, R., and Lahav, O. (2000). Massive lossless data compression and multiple parameter estimation from galaxy spectra. , 317(4):965–972.

Hermans, J., Begy, V., and Louppe, G. (2019). Likelihood-free MCMC with Amortized Approximate Ratio Estimators. *arXiv e-prints*, page arXiv:1903.04057.

Ho, M., Bartlett, D. J., Chartier, N., Cuesta-Lazaro, C., Ding, S., Lapel, A., Lemos, P., Lovell, C. C., Makinen, T. L., Modi, C., Pandya, V., Pandey, S., Perez, L. A., Wandelt, B., and Bryan, G. L. (2024). LtU-ILI: An All-in-One Framework for Implicit Inference in Astrophysics and Cosmology. *The Open Journal of Astrophysics*, 7:54.

Huang, D., Bharti, A., Souza, A., Acerbi, L., and Kaski, S. (2023). Learning Robust Statistics for Simulation-based Inference under Model Misspecification. *arXiv e-prints*, page arXiv:2305.15871.

Hyvärinen, A. and Dayan, P. (2005). Estimation of non-normalized statistical models by score matching. *Journal of Machine Learning Research*, 6(4).

Jeffrey, N. and Wandelt, B. D. (2024). Evidence Networks: simple losses for fast, amortized, neural Bayesian model comparison. *Machine Learning: Science and Technology*, 5(1):015008.

Jeffrey, N., Whiteway, L., Gatti, M., Williamson, J., Alsing, J., Porredon, A., Prat, J., Doux, C., Jain, B., Chang, C., Cheng, T. Y., Kacprzak, T., Lemos, P., Alarcon, A., Amon, A., Bechtol, K., Becker, M. R., Bernstein, G. M., Campos, A., Rosell, A. C., Chen, R., Choi, A., DeRose, J., Drlica-Wagner, A., Eckert, K., Everett, S., Ferté, A., Gruen, D., Gruendl, R. A., Herner, K., Jarvis, M., McCullough, J., Myles, J., Navarro-Alsina, A., Pandey, S., Raveri, M., Rollins, R. P., Rykoff, E. S., Sánchez, C., Secco, L. F., Sevilla-Noarbe, I., Sheldon, E., Shin, T., Troxel, M. A., Tutusaus, I., Varga, T. N., Yanny, B., Yin, B., Zuntz, J., Aguena, M., Allam, S. S., Alves, O., Bacon, D., Bocquet, S., Brooks, D., da Costa, L. N., Davis, T. M., De Vicente, J., Desai, S., Diehl, H. T., Ferrero, I., Frieman, J., García-Bellido, J., Gaztanaga, E., Giannini, G., Gutierrez, G., Hinton,

S. R., Hollowood, D. L., Honscheid, K., Huterer, D., James, D. J., Lahav, O., Lee, S., Marshall, J. L., Mena-Fernández, J., Miquel, R., Pieres, A., Malagón, A. A. P., Roodman, A., Sako, M., Sanchez, E., Sanchez Cid, D., Smith, M., Suchyta, E., Swanson, M. E. C., Tarle, G., Tucker, D. L., Weaverdyck, N., Weller, J., Wiseman, P., and Yamamoto, M. (2024). Dark Energy Survey Year 3 results: likelihood-free, simulation-based wCDM inference with neural compression of weak-lensing map statistics. .

Karchev, K. and Trotta, R. (2024). STAR NRE: Solving supernova selection effects with set-based truncated auto-regressive neural ratio estimation. *arXiv e-prints*, page arXiv:2409.03837.

Kelly, R. P., Warne, D. J., Frazier, D. T., Nott, D. J., Gutmann, M. U., and Drovandi, C. (2025). Simulation-based Bayesian inference under model misspecification. *arXiv e-prints*, page arXiv:2503.12315.

Krouglova, A. N., Johnson, H. R., Confavreux, B., Deistler, M., and Gonçalves, P. J. (2025). Multifidelity Simulation-based Inference for Computationally Expensive Simulators. *arXiv e-prints*, page arXiv:2502.08416.

Lemos, P., Coogan, A., Hezaveh, Y., and Perreault-Levasseur, L. (2023a). Sampling-Based Accuracy Testing of Posterior Estimators for General Inference. *40th International Conference on Machine Learning*, 202:19256–19273.

Lemos, P., Parker, L. H., Hahn, C., Ho, S., Eickenberg, M., Hou, J., Massara, E., Modi, C., Moradinezhad Dizgah, A., Régaldo-Saint Blancard, B., and Spergel, D. (2023b). SimBIG: Field-level Simulation-based Inference of Large-scale Structure. In *Machine Learning for Astrophysics*, page 18.

Leyde, K., Green, S. R., Toubiana, A., and Gair, J. (2024). Gravitational wave populations and cosmology with neural posterior estimation. , 109(6):064056.

Lin, K., von Wietersheim-Kramsta, M., Joachimi, B., and Feeney, S. (2023). A simulation-based inference pipeline for cosmic shear with the Kilo-Degree Survey. , 524(4):6167–6180.

Lueckmann, J.-M., Goncalves, P. J., Bassetto, G., Öcal, K., Nonnenmacher, M., and Macke, J. H. (2017). Flexible statistical inference for mechanistic models of neural dynamics. *arXiv e-prints*, page arXiv:1711.01861.

Makinen, L. T., Heavens, A., Porqueres, N., Charnock, T., Lapel, A., and Wandelt, B. D. (2025). Hybrid summary statistics: neural weak lensing inference beyond the power spectrum. , 2025(1):095.

Miller, B. K., Cole, A., Weniger, C., Nattino, F., Ku, O., and Grootes, M. W. (2022). swyft: Truncated marginal neural ratio estimation in python. *Journal of Open Source Software*, 7(75):4205.

Miller, B. K., Weniger, C., and Forré, P. (2022). Contrastive Neural Ratio Estimation for Simulation-based Inference. *arXiv e-prints*, page arXiv:2210.06170.

Papamakarios, G. and Murray, I. (2016). Fast ϵ-free Inference of Simulation Models with Bayesian Conditional Density Estimation. *arXiv e-prints*, page arXiv:1605.06376.

Papamakarios, G., Nalisnick, E., Rezende, D. J., Mohamed, S., and Lakshminarayanan, B. (2021). Normalizing flows for probabilistic modeling and inference. *Journal of Machine Learning Research*, 22(57):1–64.

Papamakarios, G., Pavlakou, T., and Murray, I. (2017). Masked autoregressive flow for density estimation. In Guyon, I., Luxburg, U. V., Bengio, S., Wallach, H., Fergus, R., Vishwanathan, S., and Garnett, R., editors, *Advances in Neural Information Processing Systems*, volume 30. Curran Associates, Inc.

Park, M., Gatti, M., and Jain, B. (2025). Dimensionality reduction techniques for statistical inference in cosmology. , 111(6):063523.

Rozet, F., Delaunoy, A., and Miller, B. (2021). Lampe: Likelihood-free amortized posterior estimation. *Statistical Software*.

Rubin, D. B. (1984). Bayesianly justifiable and relevant frequency calculations for the applied statistician. *The Annals of Statistics*, pages 1151–1172.

Saoulis, A. A., Piras, D., Spurio Mancini, A., Joachimi, B., and Ferreira, A. M. G. (2025). Full-waveform earthquake source inversion using simulation-based inference. *Geophysical Journal International*, 241(3):1740–1761.

Sharrock, L., Simons, J., Liu, S., and Beaumont, M. (2022). Sequential Neural Score Estimation: Likelihood-Free Inference with Conditional Score Based Diffusion Models. *arXiv e-prints*, page arXiv:2210.04872.

Spurio Mancini, A., Docherty, M. M., Price, M. A., and McEwen, J. D. (2023). Bayesian model comparison for simulation-based inference. *RAS Techniques and Instruments*, 2(1):710–722.

Srinivasan, R., Crisostomi, M., Trotta, R., Barausse, E., and Breschi, M. (2024). Bayesian evidence estimation from posterior samples with normalizing flows. , 110(12):123007.

Talts, S., Betancourt, M., Simpson, D., Vehtari, A., and Gelman, A. (2018). Validating Bayesian Inference Algorithms with Simulation-Based Calibration. *arXiv e-prints*, page arXiv:1804.06788.

Tejero-Cantero, A., Boelts, J., Deistler, M., Lueckmann, J.-M., Durkan, C., Gonçalves, P. J., Greenberg, D. S., and Macke, J. H. (2020). sbi: A toolkit for simulation-based inference. *Journal of Open Source Software*, 5(52):2505.

Tessore, N., Loureiro, A., Joachimi, B., von Wietersheim-Kramsta, M., and Jeffrey, N. (2023). GLASS: Generator for Large Scale Structure. *The Open Journal of Astrophysics*, 6:11.

Tortorelli, L., Siudek, M., Moser, B., Kacprzak, T., Berner, P., Refregier, A., Amara, A., García-Bellido, J., Cabayol, L., Carretero, J., Castander, F. J., De Vicente, J., Eriksen, M., Fernandez, E., Gaztanaga, E., Hildebrandt, H., Joachimi, B., Miquel, R., Sevilla-Noarbe, I., Padilla, C., Renard, P., Sanchez, E., Serrano, S., Tallada-Crespí, P., and Wright, A. H. (2021). The PAU survey: measurement of narrow-band galaxy properties with approximate bayesian computation. , 2021(12):013.

Vasist, M., Rozet, F., Absil, O., Mollière, P., Nasedkin, E., and Louppe, G. (2023). Neural posterior estimation for exoplanetary atmospheric retrieval. , 672:A147.

von Wietersheim-Kramsta, M., Lin, K., Tessore, N., Joachimi, B., Loureiro, A., Reischke, R., and Wright, A. H. (2024). KiDS-SBI: Simulation-based inference analysis of KiDS-1000 cosmic shear. , 694:A223.

Wildberger, J. B., Dax, M., Buchholz, S., Green, S. R., Macke, J., and Schölkopf, B. (2023). Flow Matching for Scalable Simulation-Based Inference. In *Machine Learning for Astrophysics*, page 34.